

The Radius Expansion Factor and Second Virial Coefficient for Polymer Chains below the Θ Temperature

Hiromi Yamakawa

Department of Polymer Chemistry, Kyoto University, Kyoto 606-01, Japan

Received May 3, 1993; Revised Manuscript Received June 22, 1993

ABSTRACT: The radius expansion factor α_S and second virial coefficient A_2 for flexible polymers below the Θ temperature are investigated within the new framework of theory recently presented. It is then shown that the (quasi-)two-parameter scheme is still valid for α_S and that the effect of chain ends can explain the observed M independence of A_2 in the range of small molecular weight M for which A_2 does not vanish at Θ . As for α_S , some aspects of the coil-to-globule transition are discussed somewhat in detail. It is also shown that, if account is taken of the ternary-cluster integral β_3 along with chain stiffness, terms involving β_3 may be neglected compared to the binary-cluster integral β_2 in α_S and A_2 , although β_3 appears separately in the third virial coefficient A_3 . Thus, the consideration of the effects of chain stiffness and chain ends along with β_2 and β_3 may give a consistent explanation of the observed behavior of α_S , A_2 , and A_3 at, above, and below Θ , while the binary-cluster approximation is actually good enough as far as only α_S and A_2 are concerned.

I. Introduction

Recently, we have started a theoretical and experimental reinvestigation¹⁻⁴ of the excluded-volume effects in dilute polymer solutions from a new point of view beyond the framework of the two-parameter theory⁵ in order to give an explanation to many experimental findings inconsistent with its prediction. The new framework, which is based on the helical wormlike (HW) chain,^{6,7} is summarized as follows. (1) The effect of chain stiffness on the radius expansion factor α_S remains large for such large molecular weight M that the ratio of the unperturbed mean-square radius of gyration $\langle S^2 \rangle_0$ to M already reaches its coil limiting value independent of M , but α_S is a function only of the scaled excluded-volume parameter \tilde{z} that takes account of both excluded-volume strength (still in the binary-cluster approximation) and chain stiffness, so that a quasi-two-parameter scheme is valid for α_S . (2) Even for large M above, the chain stiffness has a significant effect on the interpenetration function Ψ appearing in the second virial coefficient A_2 , so that Ψ is not a universal function of α_S but its change with α_S depends separately also on M and on the excluded-volume strength (or solvent power). (3) For relatively small M , the effect of chain ends on A_2 becomes appreciable, thus leading to the nonvanishing of A_2 for small M at the Θ temperature, i.e., the temperature at which it vanishes for large M ($\approx 5 \times 10^4$).

The primary object of the present paper is to examine whether in this new scheme we can or cannot explain the observed behavior of α_S and A_2 below the Θ temperature, i.e., the decrease of α_S below unity as usually called the coil-to-globule transition⁸ and the M independence of A_2 ,^{9,10} both of which have been considered to be impossible to explain by the two-parameter theory.

Now the phenomenon called the coil-to-globule transition was first suggested by Stockmayer¹¹ in 1960, and then Ptitsyn et al.¹² in 1968 were the first to treat it theoretically by taking account of the ternary-cluster integral as well as the binary-cluster one in the smoothed-density model.⁵ In fact, Orofino and Flory¹³ in 1957 had already presented such a smoothed-density (or mean-field) theory with consideration of both cluster interactions. Subsequently, following Ptitsyn, many theoreticians^{8,14,15} have pursued this line to treat the coil-to-globule transition. The corresponding theory of A_2 was also developed by Orofino and Flory¹³ and by Tanaka.¹⁶ However, the theory

of this type cannot explain the well-established experimental results that the temperature (Θ) at which A_2 vanishes is independent of M in its ordinary range (for $M \gtrsim 5 \times 10^4$)^{17,18} and that at the Θ temperature, as defined above, α_S becomes unity, or the mean-square radius of gyration $\langle S^2 \rangle$ is proportional to M for large M ($\gtrsim 10^5$).^{2,5}

In contrast to the mean-field theory above, the random-flight chain theory,¹⁹⁻²¹ which takes account of chain connectivity and both cluster integrals, predicts that α_S becomes unity at the Θ temperature since α_S and A_2 may be expressed in terms of the same effective binary-cluster integral that is a linear combination of binary- and ternary-cluster terms. Recall that the effect of chain connectivity on the latter term is quite different from that in the mean-field theory.¹⁹ As shown in section V, if the chain stiffness is further considered, its effects on the effective binary-cluster integrals in α_S and A_2 become different but the ternary-cluster terms may be neglected compared to the binary-cluster ones even for ordinary flexible polymers. This is the reason why we attempt to make an analysis of experimental data below Θ on the basis of the new framework in the binary-cluster approximation from the start. Before doing this, in the next section we consider preliminarily some aspects of the problems.

II. Preliminary Consideration of the Problems

Radius Expansion Factor. For solutions of flexible polymers, it is now known that there are two types of the coil-to-globule transitions, i.e., the gradual and sharp transitions, and that the former is observed in the stable state of the test solution, while the latter may be due to the metastable state, as claimed by Chu's group.²²⁻²⁴ Thus the present analysis is confined to the former case. Figure 1 shows plots of $\alpha_S^3|\tau|M_w^{1/2}$ against $|\tau|M_w^{1/2}$ for the data obtained by Chu's group, Miyaki, and Park et al. for polystyrene (PS) samples with different weight-average molecular weights M_w in cyclohexane with $\Theta = 34.5^\circ\text{C}$ (unfilled and half-filled circles),^{22,24,25} in methyl acetate with $\Theta = 43^\circ\text{C}$ (filled circles),²³ and in methylcyclohexane with $\Theta = 69.3^\circ\text{C}$ (triangles).²⁶ In the figure, the dashed straight line indicates the initial slope of unity, and τ is the reduced temperature defined by

$$\tau \equiv 1 - \Theta/T \quad (1)$$

with T the absolute temperature. (Note that τ is usually defined as $\tau = T/\Theta - 1$.) It is seen that the data points

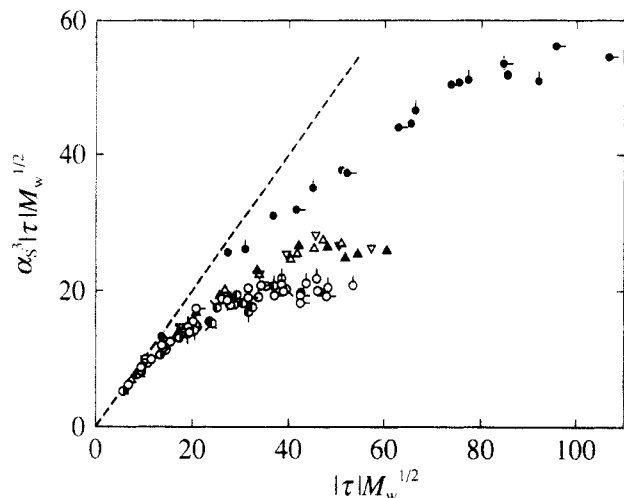


Figure 1. Plots of $\alpha_S^3 |\tau| M_w^{1/2}$ against $|\tau| M_w^{1/2}$ for PS, with τ being the reduced temperature defined by eq 1: (O with and without pips) for $460 \leq 10^{-4} M_w \leq 4090$ in cyclohexane;^{22,24} (●, ○ with and without pips) for $134 \leq 10^{-4} M_w \leq 5680$ in cyclohexane;²⁵ (● with and without pips) for $10^{-4} M_w = 200$ and 460 in methyl acetate;²³ (▽, △, ▲) for $384 \leq 10^{-4} M_w \leq 842$ in methylcyclohexane;²⁶ with the same symbols for the same M_w . The dashed straight line indicates the initial slope of unity.

for different values of M_w form a single-composite curve for each solvent, as has often been recognized.

Now the result from the mean-field theory may be written as

$$\alpha_S^5 - \alpha_S^3 - y\alpha_S^{-3} = 2.60z \quad (2)$$

where z is the conventional excluded-volume parameter in the two-parameter theory⁵ and the parameter y arises from the ternary-cluster interaction. If we assume that y is independent of M and T , then in the region of $\alpha_S \ll 1$, usually called the globule state, we have

$$\alpha_S^3 |z| \propto \alpha_S^3 |\tau| M_w^{1/2} = \text{constant} \quad (\alpha_S \ll 1) \quad (3)$$

where we have assumed as usual that the binary-cluster integral is proportional to τ .

The ordinate quantity in Figure 1 seems to level off for large $|\tau| M_w^{1/2}$, the plateau height depending on the solvent. Park et al. (Chu's group)^{22,23,26} have considered that this plateau corresponds to the globule state as represented by eq 3. However, this assumption is difficult to accept, since the experimentally accessible range is limited to $\alpha_S \gtrsim 0.7$ and it is not so small that eq 3 is valid. Nevertheless, their important finding is that, if both of the ordinate and abscissa quantities are further scaled by a constant which is inversely proportional to the plateau height, all data points for all solvents can be made to form a single-composite curve. According to eq 2, the parameter y must then be a universal constant independent of a polymer-solvent pair. This is unnatural since y arises from the ternary-cluster interaction, thus also leading to the rejection of the mean-field theory. At any rate, the implication is that the conventional two-parameter scheme may be still valid for α_S below Θ as far as the above data (for large $M_w \gtrsim 10^6$) are concerned. Recall that the effect of chain stiffness on α_S above Θ may be ignored for PS for $M_w \gtrsim 10^6$.²

Second Virial Coefficient. Figure 2 shows plots of $-A_2$ against $|\tau|$ for the data obtained by Tong et al.⁹ for PS samples with different M_w in cyclohexane below Θ . It is seen that A_2 is independent of M_w in its range displayed. The curves represent the values calculated for the indicated values of M_w from the two-parameter theory by Tanaka

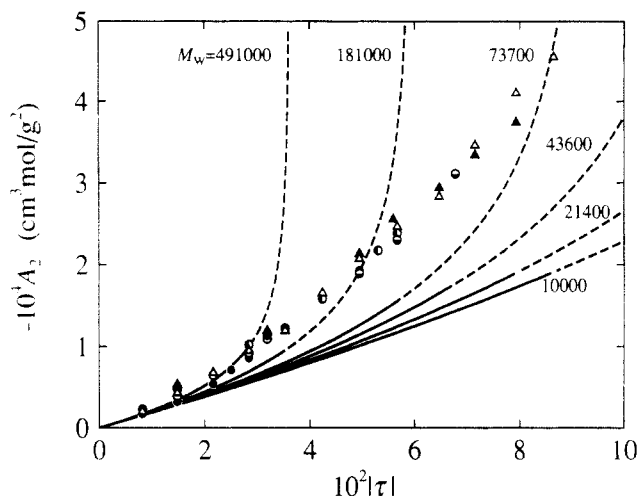


Figure 2. Plots of $-A_2$ against $|\tau|$ for PS in cyclohexane for the indicated values of M_w : (△) for $10^{-4} M_w = 1.00$; (▲) for 2.14; (●) for 4.36; (○) for 7.37; (●) for 18.1; (●) for 49.1.⁹ The curves represent the values calculated from the Tanaka-Šolc theory²⁷ with eq 4 (see the text).

and Šolc,²⁷ following Tong et al., their h function⁵ appearing in A_2 being given by

$$h(z) = (1 + 6.865z)^{-0.418} \quad (\text{TŠ}) \quad (4)$$

The solid part of each curve corresponds to the measurement range of $|\tau|$. The h function given by eq 4 has a singularity at $z = -0.1459$, so that the curves exhibit divergence. In general, the function h or Ψ (and also α_S) given by an approximate closed expression derived for $z > 0$ (in the binary-cluster approximation) has a singularity (or no solution) at $z \leq 0$. Therefore, such equations cannot be applied to the range of negative z far below Θ , and at least the dashed part of each curve in Figure 2 has no significance.

Nevertheless, it is interesting to see that there is rather good agreement between theory and experiment for $M_w = 4.91 \times 10^5$ (filled circles) and that the two-parameter theory breaks down only for smaller M_w . Thus this disagreement between theory and experiment may be regarded as arising from the effect of chain stiffness or chain ends or from both.

III. Radius Expansion Factor

We analyze the data for α_S in Figure 1 by the use of our new theory^{1,28-30} on the basis of the HW touched-bead model such that $n + 1$ beads are arrayed with spacing a between them along the contour of total length $L = na$ and that there exist excluded-volume interactions between them expressed in terms of the binary-cluster integral β . The HW model itself^{6,7} is defined in terms of the three model parameters: the constant differential-geometrical curvature κ_0 and torsion τ_0 of its characteristic helix and the static stiffness parameter λ^{-1} .

For convenience, we begin by summarizing the necessary basic equations. We assume that the radius expansion factor α_S as defined as $\alpha_S^2 = \langle S^2 \rangle / \langle S^2 \rangle_0$ is a function only of the scaled excluded-volume parameter \tilde{z} defined by

$$\tilde{z} = (3/4)K(\lambda L)z \quad (5)$$

as has already been justified experimentally above Θ .^{2,3}

where

$$K(L) = \frac{4}{3} - 2.711L^{-1/2} + \frac{7}{6}L^{-1} \quad \text{for } L > 6$$

$$= L^{-1/2} \exp(-6.611L^{-1} + 0.9198 + 0.03516L) \quad \text{for } L \leq 6 \quad (6)$$

The conventional excluded-volume parameter z is now defined by

$$z = (3/2\pi)^{3/2}(\lambda B)(\lambda L)^{1/2} \quad (7)$$

where

$$B = \beta/a^2 c_\infty^{3/2} \quad (8)$$

with

$$c_\infty = \lim_{\lambda L \rightarrow \infty} (6\lambda \langle S^2 \rangle_0 / L)$$

$$= \frac{4 + (\lambda^{-1}\tau_0)^2}{4 + (\lambda^{-1}\kappa_0)^2 + (\lambda^{-1}\tau_0)^2} \quad (9)$$

We may assume that

$$\beta = \beta_0 \tau \quad (10)$$

with β_0 being independent of T , so that

$$B = B_0 \tau \quad (11)$$

with B_0 also being independent of T . Note that $\langle S^2 \rangle_0$ is given by eq 1 of ref 1.

For $z > 0$, we adopt the Domb-Barrett expression³¹ for α_S with \bar{z} in place of z , i.e.,

$$\alpha_S^2 = [1 + 10\bar{z} + (70\pi/9 + 10/3)\bar{z}^2 + 8\pi^{3/2}\bar{z}^3]^{2/15} \times [0.933 + 0.067 \exp(-0.85\bar{z} - 1.39\bar{z}^2)] \quad (12)$$

The α_S given by eq 12 has a singularity at $\bar{z} = -0.1446$, and it cannot be applied to the range of negative \bar{z} far below Θ . At present, we do not have any appropriate closed expression for α_S that is valid for $z < 0$. Therefore, for $z < 0$, we adopt tentatively the perturbation theory,⁵

$$\alpha_S^2 = 1 + 1.276\bar{z} - 2.082\bar{z}^2 + \dots \quad (13)$$

although this series is divergent for $\bar{z} < 0$ since all the terms in powers of \bar{z} there become negative.

Next we consider a determination of B_0 , and hence z and \bar{z} , from experimental data. It is then convenient to introduce the shift factor M_L as defined as the molecular weight per unit contour length,

$$M_L = M/L \quad (14)$$

so that we have

$$z = (3/2\pi)^{3/2}(\lambda B)(\lambda/M_L)^{1/2}M^{1/2} \quad (15)$$

$$a = M_0/M_L \quad (16)$$

where M_0 is the molecular weight of the repeat unit of a given real chain, which is taken as a single bead for the present model.

We have already determined the HW model parameters for PS as follows:³² $\lambda^{-1} = 22.5 \text{ \AA}$, $M_L = 36.7 \text{ \AA}^{-1}$, and $c_\infty = 40/49$. For PS in cyclohexane, Miyaki^{25,33} has determined β_0 (per repeat unit) to be $7.2 \times 10^{-23} \text{ cm}^3$ from the data for α_S at large M_w for which \bar{z} may be equated to z , and therefore we have $\lambda B_0 = 0.54$ from eqs 8, 10, and 11. For PS in methyl acetate and in methylcyclohexane, we can determine λB_0 from the data^{23,26} for α_S near Θ (for large M_w) by the use of the first-order perturbation theory, i.e., eq 13 with $\bar{z} = z$ and with omission of the z^2 and higher

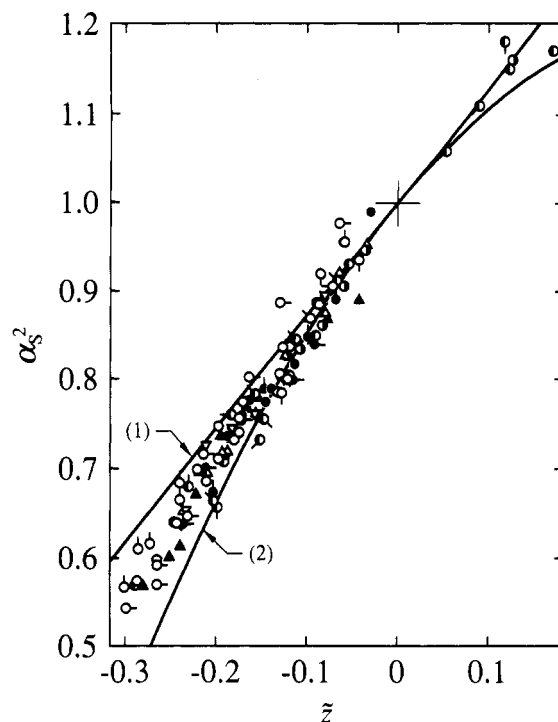


Figure 3. Plots of α_S^2 against \bar{z} for PS. The symbols have the same meaning as in Figure 1. The figure also includes the data (\bullet , \circ with and without pips) in cyclohexane above Θ .²⁵ The curves (1) and (2) represent the first- and second-order perturbation theory values, respectively, calculated from eq 13.

terms. The results are $\lambda B_0 = 0.19$ and 0.40 in methyl acetate and methylcyclohexane, respectively. Thus, for all these systems, we can calculate z at given T and M from eqs 11 and 15 and \bar{z} from eq 5 with eqs 6 and 14.

Figure 3 shows plots of α_S^2 against \bar{z} for the same data as in Figure 1. It also includes the data (half-filled circles) in cyclohexane above Θ by Miyaki.²⁵ Although for these data \bar{z} may be equated to z , we have adopted \bar{z} as the abscissa of Figure 3 for later convenience. All the data points are seen to form a single-composite curve within experimental error, indicating that the two-parameter scheme is valid, as was expected. As stated at the beginning of section II, this conclusion is valid for the *stable* solution of *flexible* polymers (except for biological macromolecules with specific intramolecular interactions). It is interesting to see that this curve, which has not been explicitly shown, lies between the solid curves (1) and (2), which have been calculated from the first- and second-order perturbation theories of eq 13, respectively. This suggests that the problem is to derive a closed expression for α_S as a function of \bar{z} or z (for $z < 0$) in the binary-cluster approximation which is consistent with its above-mentioned behavior below Θ . Note that the higher-order perturbation theories predict successively lower values of α_S for $z < 0$ since there all higher-order terms in eq 13 are negative.

With the same data as in Figure 3 (except those above Θ), the values of $\alpha_S^3|\bar{z}|$ are plotted against $|\bar{z}|$ in Figure 4, where the dashed straight line indicates the initial slope of unity. The plot corresponds to that constructed by Park et al.,^{22,23,26} and, necessarily, the data points form a single-composite curve. The solid curves (1) and (2) correspond to those in Figure 3 and either exhibits a maximum. It is therefore again difficult to consider that $\alpha_S^3|\bar{z}|$ levels off for $|\bar{z}| \gtrsim 0.2$. If so, the plot of α_S^2 vs \bar{z} in Figure 3 must clearly exhibit inflection in that range of $|\bar{z}|$. However, this is not the case. In Figure 4, the chain curve represents the values calculated from eq 2 with $z = \bar{z}$ and $y = 0.07$, although it now has no great significance. This

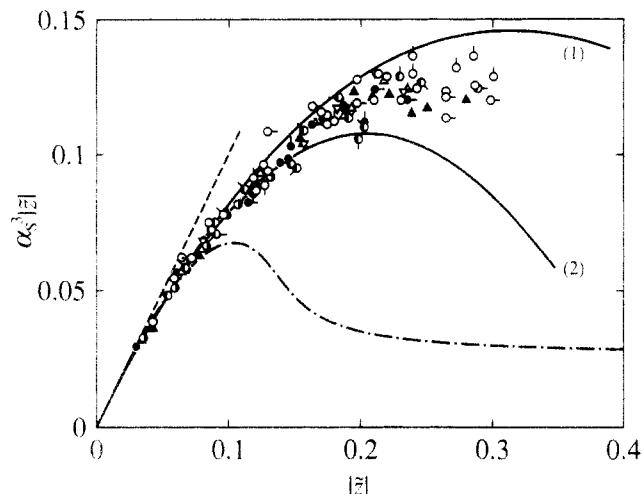


Figure 4. Plots of $\alpha_S^3|z|$ against $|z|$ for PS. The symbols have the same meaning as in Figure 1. The dashed straight line indicates the initial slope of unity. The solid curves (1) and (2) correspond to those in Figure 3, respectively. The chain curve represents the values calculated from eq 2 with $z = \bar{z}$ and $y = 0.07$.

curve also exhibits a maximum before leveling off. (Strictly, when eq 2 is fitted to the data, the values of both parameters z and y must be readjusted.) Similar results have recently been obtained by analytical calculation (with a ternary-cluster term)³⁴ and computer simulation,³⁵ both claiming that the true globule state corresponds to the plateau beyond the maximum. However, we believe that none of them can describe real polymer systems. As for the latter, note that the temperature at which A_2 vanishes depends appreciably on chain length, in contrast to the experimental results in the ordinary range of M .

IV. Second Virial Coefficient

We again begin by summarizing the necessary basic equations from the new theory^{1,28} on the basis of the same HW touched-bead model as in the last section. If the effect of chain ends is ignored, A_2 may be written in the form

$$A_2 = (N_A c_\infty)^{3/2} L^2 B / (2M^2) h \quad (17)$$

where N_A is Avogadro's number.

For $z > 0$, the h function is given by¹

$$h = (1 + 7.74\bar{z} + 52.3\bar{z}^{27/10})^{-10/27} \quad (18)$$

where

$$\bar{z} = \bar{z} / \alpha_S^3 \quad (19)$$

with

$$\bar{\bar{z}} = (Q/2.865)z \quad (20)$$

so that h is a function of \bar{z} and also another (intermolecular) scaled excluded-volume parameter $\bar{\bar{z}}$. For ordinary flexible polymers, for which $\lambda^{-1} \leq 100 \text{ \AA}$,^{6,7} Q is a function only of λL , i.e., $Q = Q(\lambda L)$. For $\lambda L \gtrsim 1$, it is given by¹

$$\begin{aligned} Q(L) = & -\frac{128\sqrt{2}}{15} - 2.531L^{-1/2} - 2.586L^{-1} + 1.985L^{-3/2} - \\ & 1.984L^{-2} - 0.9292L^{-5/2} + 0.1223L^{-3} + \frac{8}{5}x^{5/2} + \\ & \frac{2}{3}\left(8 + \frac{1}{6}L^{-1}\right)x^{3/2} + (8 - 13.53L^{-1} + 0.2804L^{-2})x^{1/2} + \\ & (-0.3333L^{-1} + 5.724L^{-2} - 0.7974L^{-3})x^{-1/2} + \\ & (-0.3398L^{-2} + 0.7146L^{-3})x^{-3/2} \quad (21) \end{aligned}$$

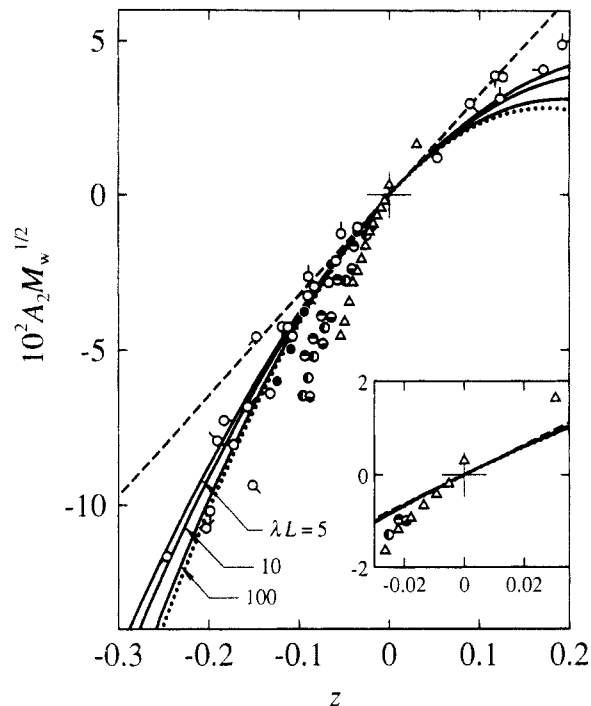


Figure 5. Plots of $A_2 M_w^{1/2}$ against z for PS in cyclohexane. The symbols have the same meaning as in Figure 2. The figure also includes the data (O with and without pips)²⁶ for $134 \leq 10^{-4} M_w \leq 3920$ below and above Θ and those (Δ) for $10^{-4} M_w = 1.00$ at 34.5 (Θ)³⁷ and 50.0 °C,⁴ with the same symbols for the same M_w . The dashed straight line has a slope of 0.323 corresponding to the leading term of eq 25. The solid curves represent the values calculated for the indicated values of λL from eq 25 with the first-order perturbation theory of h given by eq 23, the dotted curve indicating the corresponding two-parameter coil limit of $\lambda L \rightarrow \infty$. The inset is an enlargement of the region near $z = 0$.

with

$$x = 1 + 0.961L^{-1} \quad (22)$$

Note that Q has not been derived for $\lambda L \lesssim 1$ and that in the coil (two-parameter) limit of $\lambda L \rightarrow \infty$ the h function given by eq 18 is close to the Barrett function.³⁶

The function h given by eq 18 has a singularity at $z = 0$, and therefore we again adopt the perturbation theory for $z < 0$. If we simply assume that the expansion factor for each of the chains in contact is also given by a function only of \bar{z} , then we have, from the conventional two-parameter perturbation theory,^{5,27}

$$h = 1 - 2.865\bar{\bar{z}} + 8.851\bar{\bar{z}}^2 + 5.077\bar{\bar{z}}\bar{z} - \dots \quad (23)$$

with \bar{z} and $\bar{\bar{z}}$ in place of the intra- and intermolecular excluded-volume parameters z , respectively.

Now, for the present purpose, it is convenient to consider the quantity $A_2 M^{1/2}$, which may be written, from eq 17, as

$$A_2 M^{1/2} = 4(\pi/6)^{3/2} N_A (c_\infty / \lambda M L)^{3/2} z h \quad (24)$$

In the case of PS, for which the HW model parameters are given above, eq 24 reduces to

$$A_2 M^{1/2} = 0.323zh \quad (\text{PS}) \quad (25)$$

where A_2 has been expressed in $\text{cm}^3 \cdot \text{mol} / \text{g}^2$.

With the data of Figure 2 for PS in cyclohexane, the values of $A_2 M_w^{1/2}$ are plotted against z (not \bar{z} nor $\bar{\bar{z}}$) in Figure 5, where the variation of z is to be considered to arise from that of τ at constant M_w (or L). The figure also includes Miyaki's data (unfilled circles)²⁶ for $M_w > 10^6$ below and above Θ and our recent data (triangles) for M_w

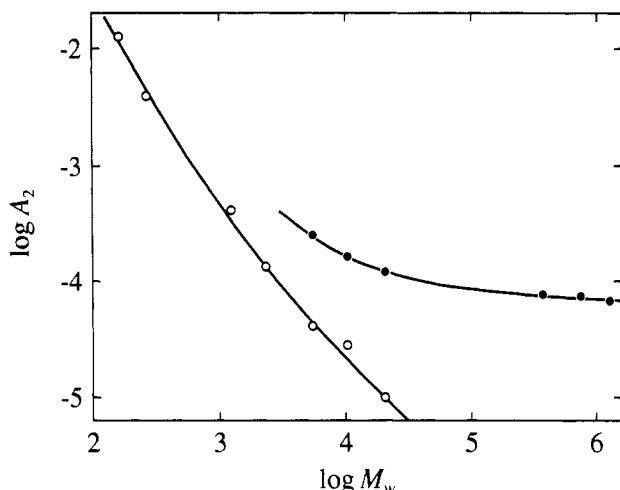


Figure 6. Double-logarithmic plots of A_2 against M_w for PS in cyclohexane: (O) at 34.5 °C;³⁷ (●) at 50.0 °C.⁴

= 10^4 at 34.5 (Θ)³⁷ and 50.0 °C,⁴ but the data by Tong et al.⁹ for $M_w = 2.14 \times 10^4$ (filled triangles in Figure 2) have been removed to avoid complication. In the figure, the dashed straight line has a slope of 0.323 corresponding to the leading term of eq 25, and the solid curves represent the values calculated for the indicated values of λL from eq 25 with the first-order perturbation theory of h given by eq 23, the dotted curve indicating the corresponding two-parameter coil limit of $\lambda L \rightarrow \infty$ (for which $\bar{z} = \bar{z} = z$). It is interesting to see that the data points for $M_w \gtrsim 5 \times 10^5$ below Θ form, within experimental error, a single-composite curve, which is nearly consistent with the above first-order two-parameter perturbation theory prediction (dotted curve), indicating that the effect of chain stiffness may be ignored there.

As seen from Figure 5, the effect of chain stiffness increases as the chain length is decreased, being such that the curve of $A_2 M_w^{1/2}$ vs z approaches the dashed line with decreasing λL . This result is rather reasonable since the chain stiffness must make α_S and therefore also h close to unity at a given z , and this direction remains unchanged even if we consider the second-order perturbation theory of eq 23. However, the observed variation of $A_2 M_w^{1/2}$ with τ (temperature) is seen to deviate more and more from the dotted curve in the opposite direction as M_w is decreased for $M_w < 5 \times 10^5$. Therefore, this behavior, or the M independence of A_2 below Θ as displayed in Figure 2, cannot be considered to arise from chain stiffness.

Now it is clearly seen from the inset of Figure 5 that, for $M_w = 10^4$, A_2 does not vanish at $T = \Theta$ ($z = 0$) but is definitely positive there, as has sometimes been recognized in light scattering (LS)³⁸ and small-angle X-ray scattering (SAXS)^{32,39} measurements for small M_w ($\lesssim 5 \times 10^4$), and that $A_2 M_w^{1/2}$ increases with increasing z (temperature) along a curve which crosses the dashed line at a certain negative value of z . It is therefore reasonable to consider that the above behavior of A_2 below Θ is closely related to its nonvanishing at Θ . As for the latter, we have already made a preliminary analysis¹ of our SAXS data,^{32,39} taking account of the effect of chain ends. In Figure 6, we show our recent data^{4,37} for A_2 from LS measurements, which are more reliable than those from SAXS, for PS samples with different M_w in cyclohexane at 34.5 (Θ) and 50.0 °C. (Note that the two of these data at $M_w = 10^4$ have been plotted in Figure 5.) Indeed, it is seen that A_2 increases rather sharply with decreasing M_w for $M_w \lesssim 10^5$ at 50.0 °C as well as at Θ , indicating that the effect of chain ends remains in such a range of M_w even above Θ . This may be expected to be the case also below Θ .

It is then helpful to consider the situation somewhat quantitatively. According to the previous analysis,¹ A_2 in general may be written in the form

$$A_2 = A_2^{(HW)} + a_1 M^{-1} + a_2 M^{-2} \quad (26)$$

where the a_1 and a_2 terms are due to the effect of chain ends, and $A_2^{(HW)}$, which vanishes at Θ , is the part of A_2 without this effect and may simply be regarded as the two-parameter theory A_2 at present. The data of Figure 6 may then be explained by taking $a_1 > 0$ and $a_2 \gtrsim 0$ at $T \geq \Theta$ (see Figure 3 of ref 1). The M independence of A_2 below Θ (or its behavior in Figure 5) implies that a_1 vanishes at a certain temperature below Θ and becomes negative for lower temperatures. Note that the deviation of $A_2 M^{1/2}$ due to this effect is of order $M^{-1/2}$. A detailed analysis of the data of Figure 6 and also those in a good solvent will be made elsewhere,³⁷ taking account of the effect of chain ends.

V. Concluding Remarks

Our problem is now reduced to a derivation of closed expressions for α_S and h (as functions of z) in the binary-cluster approximation that can be applied to the range of negative z , as far as we consider the stable solution of flexible polymers except for biological macromolecules with specific intramolecular interactions. This is a difficult future problem. However, we only note here that in this derivation the effect of chain stiffness below Θ must be reconsidered so that it may prevent the chain from collapsing without limit. Thus, in this section, we show that the ternary-cluster terms in α_S and A_2 may be neglected if the chain stiffness is taken into consideration.

By an application of the general formulation for the random-flight chain with binary- and ternary-cluster interactions¹⁹ to the HW chain,^{1,28,30,40} it can easily be shown that the effective binary-cluster integrals, which we here designate by β , appearing in α_S and A_2 may be written in the form

$$\beta = \beta_2 + \beta_3' \quad (27)$$

with

$$\beta_3' = C(\lambda a)^2(\beta_3/a^3) \quad (28)$$

where β_2 and β_3 are the (actual) binary- and ternary-cluster integrals, respectively, and C are numerical constants at most of order unity but different in α_S and A_2 . In the random-flight chain limit of $\lambda a = 1$, eq 27 with eq 28 reduces to the previous result¹⁹ with $C = 4(3/2\pi)^{3/2}$. On the other hand, in the stiff chain limit of $\lambda a \rightarrow 0$, β_3' may be completely neglected, so that $\beta = \beta_2$. This result is reasonable since the probability of multiple bead contact associated with β_3 is much smaller than that of the corresponding single contact associated with β_2 .

For ordinary flexible chains, β_3' may still be neglected compared to β_2 since $0.01 \lesssim \lambda a \lesssim 0.2$. In fact, for PS in cyclohexane at 34.5 °C (Θ), β_3 (per repeat unit) is found to be 4.7×10^{-45} cm⁶ from the observed value of the third virial coefficient A_3 ,¹⁷ so that β_3' is estimated to be 0.33×10^{-23} cm³, which is only at most 5% of β_0 ($= 7.2 \times 10^{-23}$ cm³), if the temperature dependence of β_3 is neglected and C is simply taken as unity. (The difference between the β 's in α_S and A_2 must then be negligibly small, if any.) Note that Nakamura et al.¹⁷ have erroneously put $\lambda a = 1$ in eq 28 (see ref 15 of their paper) and that for the random-flight (or Gaussian) bead model the cut-off parameter, σ ,^{17,21} must be set equal to unity;¹⁹ the effect of larger σ must be taken into account explicitly by chain stiffness.

It has now been shown that the consideration of the effects of chain stiffness and chain ends along with the binary- and ternary-cluster integrals may give a consistent explanation of the observed behavior of α_S , A_2 , and A_3 at, above, and below Θ ,⁴¹ while the binary-cluster approximation is actually good enough as far as only α_S and A_2 are concerned. Even with binary- and ternary-cluster interactions, the mean-field theory fails to explain all experimental results, as frequently mentioned above. Indeed, nearly 30 years ago, we already abandoned such an approach in the field of dilute polymer solution theory.^{5,19} Thus our new framework of theory may in principle resolve almost all fundamental problems⁴² that have remained unsolved in the field of classical dilute polymer solution science.

Acknowledgment. The author has benefited from numerous discussions with Dr. Y. Einaga.

References and Notes

- (1) Yamakawa, H. *Macromolecules* **1992**, *25*, 1912.
- (2) Abe, F.; Einaga, Y.; Yoshizaki, T.; Yamakawa, H. *Macromolecules* **1993**, *26*, 1884.
- (3) Abe, F.; Einaga, Y.; Yamakawa, H. *Macromolecules* **1993**, *26*, 1891.
- (4) Yamakawa, H.; Abe, F.; Einaga, Y. *Macromolecules* **1993**, *26*, 1898.
- (5) Yamakawa, H. *Modern Theory of Polymer Solutions*; Harper & Row: New York, 1971.
- (6) Yamakawa, H. *Annu. Rev. Phys. Chem.* **1984**, *35*, 23.
- (7) Yamakawa, H. In *Molecular Conformation and Dynamics of Macromolecules in Condensed Systems*; Nagasawa, M., Ed.; Elsevier: Amsterdam, The Netherlands, 1988; p 21.
- (8) Williams, C.; Brochard, F.; Frisch, H. L. *Annu. Rev. Phys. Chem.* **1981**, *32*, 433.
- (9) Tong, Z.; Ohashi, S.; Einaga, Y.; Fujita, H. *Polym. J.* **1983**, *15*, 835.
- (10) Perzynski, R.; Delsanti, M.; Adam, M. *J. Phys.* **1987**, *48*, 115.
- (11) Stockmayer, W. H. *Makromol. Chem.* **1960**, *35*, 54.
- (12) Ptitsyn, O. B.; Kron, A. K.; Eizner, Y. Y. *J. Polym. Sci., Part C* **1968**, *16*, 3509.
- (13) Orofino, T. A.; Flory, P. J. *J. Chem. Phys.* **1957**, *26*, 1067.
- (14) de Gennes, P.-G. *J. Phys. Lett.* **1975**, *36*, L55.
- (15) Sanchez, I. C. *Macromolecules* **1979**, *12*, 980.
- (16) Tanaka, F. *J. Chem. Phys.* **1985**, *82*, 4707.
- (17) Nakamura, Y.; Norisuye, T.; Teramoto, A. *Macromolecules* **1991**, *24*, 4904.
- (18) Norisuye, T.; Fujita, H. *Chemtracts: Macromol. Chem.* **1991**, *2*, 293.
- (19) Yamakawa, H. *J. Chem. Phys.* **1966**, *45*, 2606.
- (20) Cherayil, B. J.; Douglas, J. F.; Freed, K. F. *J. Chem. Phys.* **1985**, *83*, 5293.
- (21) Norisuye, T.; Nakamura, Y. *Polymer* **1993**, *34*, 1440.
- (22) Park, I. H.; Wang, Q.-W.; Chu, B. *Macromolecules* **1987**, *20*, 1965.
- (23) Chu, B.; Park, I. H.; Wang, Q.-W.; Wu, C. *Macromolecules* **1987**, *20*, 2833.
- (24) Park, I. H.; Fetters, L.; Chu, B. *Macromolecules* **1988**, *21*, 1178.
- (25) Miyaki, Y. Ph.D. Thesis, Osaka University, Osaka, Japan, 1981.
- (26) Park, I. H.; Kim, J.-H.; Chang, T. *Macromolecules* **1992**, *25*, 7300.
- (27) Tanaka, G.; Šolc, K. *Macromolecules* **1982**, *15*, 791.
- (28) Yamakawa, H.; Stockmayer, W. H. *J. Chem. Phys.* **1972**, *57*, 2843.
- (29) Yamakawa, H.; Shimada, J. *J. Chem. Phys.* **1985**, *83*, 2607.
- (30) Shimada, J.; Yamakawa, H. *J. Chem. Phys.* **1986**, *85*, 591.
- (31) Domb, C.; Barrett, A. J. *Polymer* **1976**, *17*, 179.
- (32) Konishi, T.; Yoshizaki, T.; Saito, T.; Einaga, Y.; Yamakawa, H. *Macromolecules* **1990**, *23*, 290.
- (33) Miyaki, Y.; Fujita, H. *Macromolecules* **1981**, *14*, 742.
- (34) Grosberg, A. Yu.; Kuznetsov, D. V. *Macromolecules* **1992**, *25*, 1996.
- (35) Szleifer, I.; O'Toole, E. M.; Panagiotopoulos, A. Z. *J. Chem. Phys.* **1992**, *97*, 6802.
- (36) Barrett, A. J. *Macromolecules* **1985**, *18*, 196.
- (37) Einaga, Y.; Abe, F.; Yamakawa, H. *Macromolecules*, to be submitted.
- (38) Huber, K.; Stockmayer, W. H. *Macromolecules* **1987**, *20*, 1400.
- (39) Tamai, Y.; Konishi, T.; Einaga, Y.; Fujii, M.; Yamakawa, H. *Macromolecules* **1990**, *23*, 4067.
- (40) Shimada, J.; Yamakawa, H. *Macromolecules* **1984**, *17*, 689.
- (41) For a detailed discussion of A_3 above Θ , see: Norisuye, T.; Nakamura, Y.; Akasaka, K. *Macromolecules*, in press.
- (42) Fujita, H. *Polymer Solutions*; Elsevier: Amsterdam, The Netherlands, 1990.